JOURNAL OF MATERIALS SCIENCE (2005)

Fabrication of $(TiB_2 - TiC)_p$/AZ91 magnesium matrix hybrid composite

B. X. MA, H. Y. WANG, Y. WANG, Q. C. JIANG*
Key Laboratory of Automobile Materials of Ministry of Education and Department of Materials Science and Engineering,Jilin University at Nanling Campus, No. 142 Renmin Street, Changchun, 130025, People's Republic of China
E-mail: jqc@jlu.edu.cn

Magnesium MMCs reinforced with TiB_2−TiC particulates were fabricated successfully via a master alloy route using a low cost Al-Ti-B_4C system as starting material system. Microstructural characterization of the (TiB_2−TiC)/AZ91 composite shows relatively uniform distribution of TiB_2 and TiC particulates in the matrix material. Moreover, the results show that the hardness and wear resistance of the composites are higher than those of the unreinforced AZ91 alloy. © *2005 Springer Science + Business Media, Inc.*.

Magnesium metal matrix composites (MMCs) have a great potential to apply to automobile, aerospace industries since the density of magnesium is low as compared with other metal alloys and the composite is expected to achieve excellent mechanical, physical and thermal properties [1, 2]. In particular, hard ceramic particles reinforced magnesium MMCs are of more interest due to their ease of fabrication, lower costs, and more isotropic properties by comparison with fiber reinforced composites [3, 4]. It is widely recognized that the properties of MMCs are controlled by the size and volume fraction of the reinforcement phases as well as by the nature of the matrix-reinforcement interfaces [5–7]. To improve the interfacial compatibility and reduce the reinforcement size, various new processing techniques are being employed to fabricate the high performance composites. Currently, MMCs produced using the various conventional routes sometimes suffer from the thermodynamic instability of interfaces between reinforcement and matrix [8]; furthermore, the scale of the reinforcing phase is limited by the starting powder size, which is typically of the order microns to tens of microns and rarely low 1 μm [4–6]. As a result of the limitations of these ex situ processes, an innovative *in situ* process via chemical reactions leading to the formation of thermodynamically stable reinforcing ceramic phase has been developed. One of these technologies is self-propagating high-temperature synthesis (SHS). It provides a number of advantages for making composites, such as a low energy requirement, cost-effectiveness, high productivity, and producing high purity products [9–11]. However, in this case, the 'inert' matrix acts as a dilute, which may cause damping of the combustion wave [3, 12]. Therefore, a more suitable and effective process method is needed in order to solve the above problems. In our previous studies, a mater alloy route, a high volume fraction SHS TiB_2-Al or TiC-Al reaction product being added to an Mg melt, has been employed to fabricate TiB_2 or TiC particulate reinforced magnesium MMCs [5, 6]. Studies on microstructures of the composites have verified that *in situ* formed and fine-size TiB_2 or TiC reinforcement particulates in the master alloy can be uniformly distributed in the magnesium matrix with clean and thermodynamically stable particulate-matrix interfaces.

Among various ceramic particles, TiB_2 and TiC are particularly attractive because of their high melting point, high hardness, good thermal shock resistance, excellent high-temperature stability, and low density [13, 14]. Recently, using the SHS reactions of Al-Ti-B or Al-Ti-C systems to synthesize TiB_2 or TiC particulates have been extensively studied by a number of researchers [15–18]. However, limited studies have been carried out on using Al-Ti-B_4C SHS reaction system to produce TiB_2 − TiC ceramics [12, 19].

In the present study, a low cost starting material system of Al-Ti-B_4C is used to fabricate *in situ* ceramic reinforcements TiB_2 − TiC. The using of Al-Ti-B_4C system provides several potential advantages. On the one hand, using B_4C as a reactant instead of pure boron, the raw material costs would be reduced since B_4C is at least 10 times less expensive than the very high cost of boron. On the other hand, using B_4C instead of pure boron or carbon may achieve the simultaneous formation of TiB_2 − TiC. Thus, it is extremely attractive to use B_4C to replace boron or carbon to synthesize TiB_2 -TiC particulates. The primary aim of the study is to examine the feasibility of fabrication of *in situ* TiB_2 − TiC particulates synthesized by using Al-Ti-B_4C as starting material system reinforced magnesium MMCs via a master alloy route.

The powder materials used for preparation of the master alloy containing *in situ* formed TiB_2 − TiC were pure titanium (99.5%, particle size less than 25 μm),

*Author to whom all correspondence should be addressed.
0022-2461
DOI: 10.1007/s10853-005-0886-2

TABLE I The main composition of the alloy

Element	Al	Zn	Mn	Si	Mg
Content (wt.%)	8.800	0.850	0.287	0.025	Bal.

aluminum (98.4%, particle size less than 27 μm) and boron carbide (98.0%, particle size less than 3.5 μm). The level for the Ti: B_4C molar ratio was 3:1, corresponding to TiB_2/TiC target ratio of 2:1. Powder blends with 40 or 60 wt.% Al were mixed dry in a cylindrical stainless steel jar containing hardened stainless steel ball by mechanical rotation at 50 rpm with a ball-to-powder weight ratio of 10:1 for 7 h, and then were uniaxially pressed into cylindrical compacts under a pressure of 20–25 MPa to obtain about 70 ± 5% theoretical densitiy. Subsequently, the compact was placed in a vacuum electrical resistance furnace to heat to about 600°C, and then the bottom surface of the compact was ignited by applying a current of about 12 A through a resistance wire. $TiB_2 - TiC$ particulates were *in situ* formed in aluminum via SHS reaction, and a master alloy containing pure aluminum and $TiB_2 - TiC$ particulates were then formed. $TiB_2 - TiC$ particulates and aluminum in the master alloy are used as reinforcement and alloying element, respectively.

The $(TiB_2 - TiC)_p$/AZ91 composites were prepared by adding the master alloy to molten magnesium and using a stirring technique. Based on the chemical compositions of AZ91 alloy (Mg-9 pct Al-1 pct Zn), commercially pure Mg, Al and Zn were selected to prepare the matrix. About 1 kg of pure magnesium was melted at 750°C in a graphite crucible in electric resistance furnace under an argon protective atmosphere. The master alloy and alloying elements were wrapped in aluminum foil and then introduced into the magnesium melt, held at that temperature until the master alloy and alloying elements were dissolved. The amounts of master alloy and alloying elements added corresponded to the composition of 5 wt.% $(TiB_2 - TiC)_p$/AZ91. After dissolving, the melt was stirred with a graphite stirrer for about 30 min to assist the dispersion of the ceramic particulates into the magnesium matrix and then, poured into an iron mould to cast the composites casting. The main composition of the alloy is given in Table I.

Microstructure and phase analyses of the master alloys and magnesium MMCs were investigated by using scanning electron microscopy (SEM) (Model SHIMADZA, SSX-550, Japan) equipped with energy-dispersive X-Ray spectrum (EDX) (Model SHIMADZA, SEDX-550, Japan) and X-Ray diffraction (XRD) (Model D/Max 2500PC Rigaku, Japan).

During the process of SHS reaction, Ti, B_4C and Al may interact to form desired $TiB_2 - TiC$ ceramic particulates. However, the chemical reaction taking place during this process is essential, because it is of interest to help to understand the reaction mechanisms of the system. Therefore, it is necessary to study the thermodynamics of the system to determine the possibility of some reactions during the *in situ* synthesis process. During the *in situ* reaction, the following three reactions

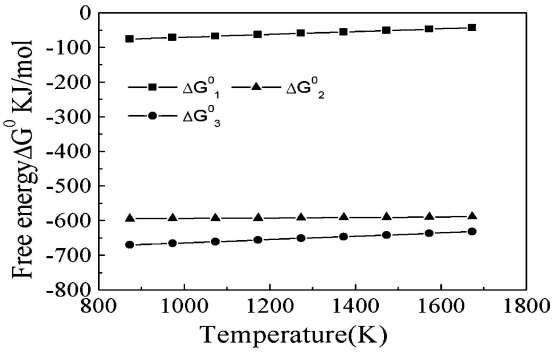

Figure 1 Changes of standard of Gibbs free energy as a temperature for $\Delta G^0{}_1$, ΔG_2^0 and ΔG_3^0.

are possible to occur:

$$3Al + Ti \rightarrow Al_3Ti$$
$$\Delta G_1^0 = -37023 + 13.533T \text{ J/mol} \quad (1)$$
$$3Al_3Ti + B_4C \rightarrow 2\,TiB_2 + TiC + 9\,Al$$
$$\Delta G_2^0 = -601230 + 7.391T \text{ J/mol} \quad (2)$$
$$3\,Ti + B_4C \rightarrow 2TiB_2 + TiC$$
$$\Delta G_3^0 = -712300 + 47.99T \text{ J/mol} \quad (3)$$

Based on available thermodynamic data [20], the change in standard Gibbs free energy ΔG^0 for each reaction is calculated and shown in Fig. 1 as a function of temperature. It can be observed that the changes in standard Gibbs free energy of three reactions are all negative, which indicates that the above reactions are all favorable. It is worth noting that ΔG_3^0 is more negative for the formation of $TiB_2 - TiC$ in the temperature range of interest, and thus reaction (3) has a higher tendency for the formation of $TiB_2 - TiC$ than of the other two reactions. Therefore, it can be deduced that the finial equilibrium phases should be TiB_2, TiC and Al in the SHS products of Al-Ti-B_4C system. However, it is of interest to note that, near the melting point of aluminum, the reaction for Al_3Ti formation is more favorable, kinetically, and hence occurs initially. This may subsequently initiate the reactions between Al_3Ti or Ti and B_4C by the heat liberation of the reaction. This proposal is consistent with the experimental results of Gotman *et al*. [12] and Nassaj *et al*. [19].

SEM micrograph and XRD pattern of the $(TiB_2 + TiC)$-Al master alloy synthesized by a 40 wt.% Al-Ti-B_4C system are shown in Fig. 2a and b, respectively. Apparently, except for the TiB_2, TiC and Al phases, no other interphases were found in the master alloy. It is consistent with the calculated result of thermodynamics. Furthermore, the XRD result shows that TiB_2 and TiC are simultaneously formed in the master alloy. The diffraction peaks for TiB_2 are more intense than those for TiC. This was expected given the reactant compositions. By metallographic observation of Fig. 2a, three types of particulates can be seen, namely, hexagonal or rectangular, and near-spherical shaped particulates. TiB_2 is present typically as hexagonal prisms or rectangular shape while TiC is irregular but near-spherical [5, 6]. These shapes of *in situ* TiB_2 and TiC are

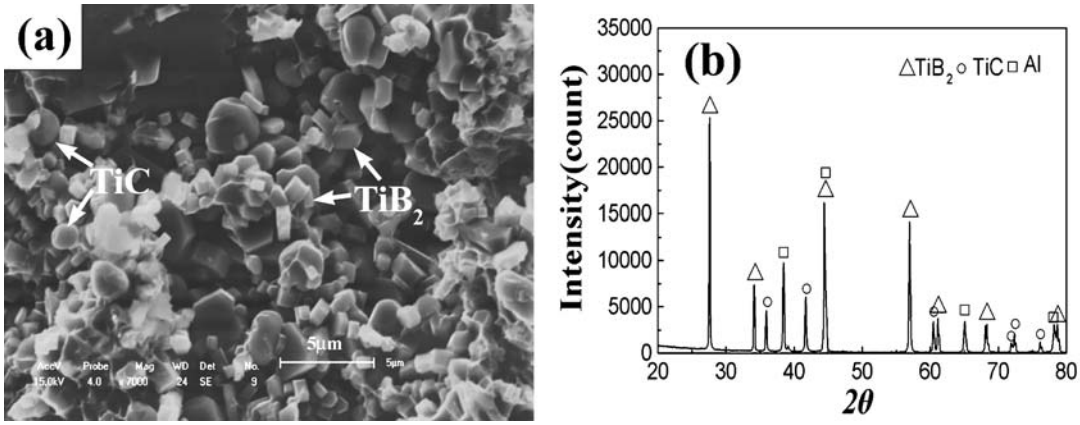

Figure 2 (a) SEM microstructure and (b) XRD pattern of the master alloy synthesized by a 40 wt.% Al-Ti-B_4C system.

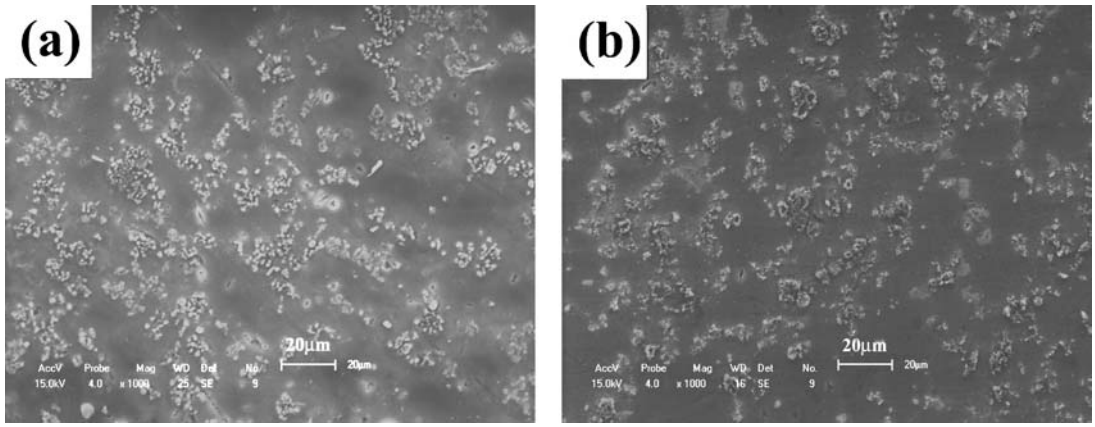

Figure 3 SEM microstructures of 5.5 wt.% $(TiB_2 - TiC)_p$/AZ91 composites fabricated by adding $(TiB_2 + TiC)$-Al master alloys with (a) 40 and (b) 60 wt.% Al.

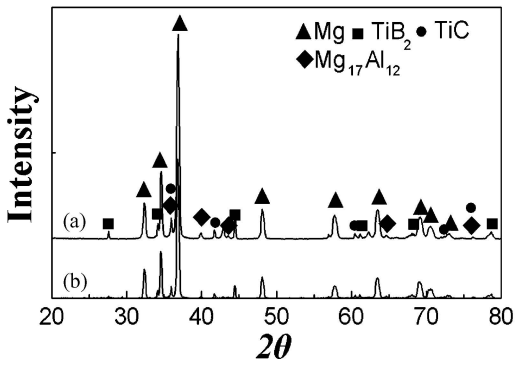

Figure 4 XRD patterns of 5.5 wt.% $(TiB_2 - TiC)_p$/AZ91 composites fabricated by adding $(TiB_2 + TiC)$-Al master alloys with (a) 40 and (b) 60 wt.% Al.

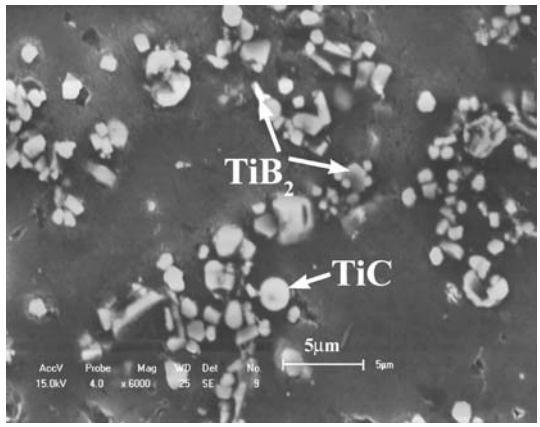

Figure 5 High magnification SEM micrograph of the 5.5 wt.% $(TiB_2 - TiC)_p$/AZ91 composite fabricated by adding $(TiB_2 + TiC)$-Al master alloy with 40 wt.% Al.

similar to those observed for Al-Ti-B and Al-Ti-C systems [6, 21]. Furthermore, the *in situ* formed TiB_2 and TiC particulates were very fine. The size of the hexagonal prisms is typically 2 μm in length and 1.5 μm in thickness. Some smaller particulates of TiB_2 and TiC of size ranging from 0.8 to 1 μm can also be seen.

Quantitative assessment of the TiB_2 and TiC particulates in the Mg composite after fabrication was carried out using the chemical dissolution. The composite sample was dissolved in a 36–38% hydrochloric acid solution, followed by filtering the suspension, and therefore, the TiB_2 and TiC particulates were then extracted. The results of the chemical dissolution tests indicate that, after fabrication, the weight fraction of the TiB_2 and TiC particulates in the Mg composite is 5.5%, and is slightly higher than that as designed. This may be associated with oxidation and burning loss of Mg melt during the processing. Figs. 3 and 4 show the SEM micrographs and XRD patterns of 5.5 wt.% $(TiB_2 - TiC)_p$/AZ91 composites fabricated by adding a (TiB_2+TiC)-Al master alloy processed via SHS reaction in 40 and 60 wt.% Al-Ti-B_4C systems into molten magnesium alloy and using the stir casting technique, respectively. According to the XRD patterns, both the

TABLE II Hardness and volumetric wear rates of the AZ91 alloy and the $(TiB_2 - TiC)_p$/5.5 wt.% $(TiB_2 - TiC)$/AZ91 composite

Material	Hardness (HB)	Volumetric wear rate (10^{-10} m^3/m) 5*N*	35*N*
AZ91 alloy	56	6.1166	19.9389
$(TiB_2 - TiC)_p$/AZ91 composite	79	2.6509	9.9477

composites consist of Mg phase, TiB_2 and TiC particulates, and $M_{17}Al_{12}$ eutectic phase. As can be observed in Fig. 3, the TiB_2 and TiC particulates with the size and morphology that are similar to those in master alloy are distributed homogeneously relatively in the Mg matrix. A high magnification SEM micrograph in Fig. 5 may exhibit more clearly hexagonal or rectangular TiB_2 and near-spherical TiC; however, some smaller TiB_2 and TiC particulates in the composite microstructure are difficult to be distinguished due to their fine sizes.

Hardness and volumetric wear rates of the unreinforced AZ91 alloy and $(TiB_2 - TiC)_p$/AZ91 composite are listed in Table II. The sliding abrasive wear rates were tested under contact loads of 5N and 35N at a constant sliding using a pin-on-disc apparatus. Both the unreinforced AZ91 alloy and $(TiB_2 - TiC)_p$/AZ91 composite were used as pin materials with 6 mm diameter and 12 mm height, and 1000 grit SiC abrasive papers (corresponding to 15 μm abrasive particles) were used as the counterface. It is apparent that the hardness and wear resistance of the $(TiB_2 - TiC)_p$/AZ91 composite are higher than those of the unreinforced AZ91 alloy as expected. It can be concluded that the presence of TiB_2 and TiC particulates has a significant improvement in the hardness and wear resistance of the composite.

Based on the above experimental results, it can be concluded that the magnesium MMCs reinforced with $TiB_2 - TiC$ particulates were successfully fabricated via a master alloy route using a low cost Al-Ti-B_4C system.

Acknowledgements

This work is supported by The National Natural Science Foundation of China (No. 50171029 and 50371030) and The Natural Science Foundation of Jilin (No. 20030503-2).

References

1. T. IMAI, S. W. LIM, D. JIANG and Y. NISHIDA, *Scripta. Mater.* **36** (1997) 611.
2. S. W. LIM, T. IMAI, Y. NISHIDA and T. CHOH, *Scripta. Metall. Mater.* **32** (1995) 1713.
3. S. C. TJONG and Z. Y. MA, *Mater. Sci. Eng.* A **29** (2000) 49.
4. X. C. TONG and H. S. FANG, *Metall. Mater. Trans.* A **29** (1998) 875.
5. Q. C. JIANG, X. L. LI and H. Y. WANG, *Scripta. Mater.* **48** (2003) 713.
6. H. Y. WANG, Q. C. JIANG, Y. Q. ZHAO, F. ZHAO, B. X. MA and Y. WANG, *Mater. Sci. Eng.* A **372** (2004) 109.
7. I. H. SONG, D. K. KIM, Y. D. HAHN and H. D. KIM, *Scripta. Mater.* **48** (2003) 1349.
8. M. A. MATIN, L. LU and M. GUPTA, *ibid.*. **45** (2001) 479.
9. P. LI, E. G. KANDALOVA, V. I. NIKITIN, A. G. MAKARENKO, A. R. LUTS and Y. F. ZHANG, *ibid.*. **49** (2003) 699.
10. J. J. MOORE and H. J. FENG, *Prog. Mater. Sci.* **39** (1995) 243.
11. J. SUBRAHMANYAM and M. VIJAYAKUMAR, *J. Mater. Sci.* **27** (1992) 6249.
12. I. GOTMAN and M. J. KOCZAK, *Mater. Sci. Eng.* A **187** (1994) 189.
13. G. WEN, S. B. LI, B. S. ZHANG and Z. X. GUO, *Acta. Mater.* **49** (2001) 1463.
14. I. SONG, L. WANG and M. WIXOM, *J. Mater. Sci.* **35** (2000) 2611.
15. H. J. BRINKMAN, J. DUSZCZYK and L. KATGERMAN, *Scripta. Mater.* **37** (1997) 293.
16. K. L. TEE, L. LU and M. O. LAI, *Mater. Sci. Eng.* A **339** (2003) 227.
17. Z. H. ZHANG, X. F. BIAN, Z. Q. WANG, X. F. LIU and Y. WANG, *J. Alloy. Compd.* **339** (2002) 180.
18. M. K. PREMKUMAR and M. G. CHU, *Metall. Trans.* A **24** (1993) 2358.
19. E. T. NASSAJ, M. KOBASHI and T. CHOH, *Scripta. Mater.* **37** (1997) 605.
20. Y. J. LIANG and Y. C. CHE, Data Handbook of Mineral Thermodynamics, edited by Northeastern University Press, 1993 (in China).
21. K. L. TEE, L. LU and M. O. LAI, *Compos. Struct.* **47** (1999) 589.

Received 2 September 2004
and accepted 8 March 2005